**Investigating the Effect of Construction Activities on Lightweight Cellular Concrete Subbase Pavements**

Abimbola Grace Oyeyi, Ph.D. Candidate, Department of Civil and Environmental Engineering University of Waterloo

Frank Mi-Way Ni, Ph.D, Post Doctoral Fellow, Department of Civil and Environmental Engineering University of Waterloo

Brad Dolton, P.Eng Manager, Geotechnical Solutions, CEMATRIX Corporation

Susan L. Tighe, FCSE, Ph.D, P.Eng

Provost and Vice-President (Academic) McMaster University, Professor of Civil Engineering

Paper prepared for presentation at the Innovations in Pavement Management, Engineering and Technologies Session of the 2022 TAC Conference & Exhibition, Edmonton, AB

**Acknowledgments**:

The authors would like to thank the Region of Waterloo, CEMATRIX Canada, E&E Seegmiller, and the Centre for Pavement and Transportation Technology (CPATT), University of Waterloo, for supporting this research. Funding for this research is in part provided by CEMATRIX Canada and Natural Sciences and Engineering Association of Canada (NSERC)

**Abstract**

Lightweight Cellular Concrete (LCC) is gaining popularity for its use in various construction projects. The feasibility of incorporating LCC into pavement construction has recently been investigated. This study analysed construction activities' effects on three LCC densities and granular A material to examine further the viability of employing LCC as a subbase alternative to unbound aggregate. This included designing, instrumentation, and building a four-section 200-meter field segment. A control section employed granular A as a subbase layer, while LCC400, LCC475, and LCC600 sections applied 400 kg/m³, 475 kg/m³, and 600 kg/m³ LCC as subbase, respectively. The density of LCC were chosen based on past industry experience for pavement construction. Materials applied in the other layers were the same in all four sections. Subsurface instrumentation was installed to monitor the pavement pressure, strain, moisture, and temperature response. The predicted ultimate strengths for 400, 475 and 600 kg/m³ were found to be 0.93 MPa, 1.93 MPa, and 2.08 MPa. Results also indicated that the control section experienced 78% more peak pressure than the LCC475 and LCC600 sections and 61% more pressure than the LCC400 section during construction. It was determined that a long-time frame between LCC pour and asphalt paving operation coupled with excessive truck traffic before asphalt paving could be detrimental to the performance of LCC pavements. This is due to high strain responses and damage to the LCC homogenous air bubble structure.

## 1.0 Introduction

With limited funding and competing infrastructural needs, it is important to research improving the service life of road pavements through enhanced planning, construction, and operation (Tighe et al., 2007). This will ensure that road infrastructure requirements are met while also serving their intended purpose. Understanding the behaviour of road pavement structures during construction operations is critical for developing improved plans and processes that will enhance performance while minimising damage and undesirable situations that could lead to premature failure. This is extremely significant when new materials are introduced into the pavement layers.

Recently, the use of Lightweight Cellular Concrete as a pavement subbase has gained recognition due to its many benefits, such as low weight and good insulation properties (Tiwari et al., 2017; Decký et al., 2016; Liu et al., 2022). LCC is a cementitious material consisting of cement, water, and preformed foam. In some cases, it constitutes fine aggregates and pozzolanic material such as fly ash and slag (Legatski, 1994). For below-ground applications, densities ranging between 250 and 600 kg/m³ have been deemed suitable. Previously, LCCs application as a fill material within the pavement structure has yielded many advantages and proven successful, especially in increasing the service life of pavements in areas with very weak subgrades (Decký et al., 2016; Dolton et al., 2016, Maher & Hagan, 2016; Averyanov, 2018)

However, incorporating LCC as a structural layer designed to replace the traditional subbase material is evolving. Past studies have compared analytically, pavement response of three LCC densities ranging between 400 and 600 kg/m³ with the traditional granular B material and found that incorporating LCC as a subbase could potentially provide longer service pavements by allowing between two to twenty times more traffic load of the same magnitude (Ni et al., 2021). Furthermore, an earlier field study also reflected that pavement response especially pressures experienced at the top of the subgrade, could be reduced significantly particularly in very low temperatures when comparing 475kg/m³ of LCC with a 22% greater thickness of Granular B material (Oyeyi et al., 2019). Still, no research has investigated the impact that construction activities may have on the long-term functioning of these pavements. With an awareness

that construction activities may impact the performance of LCC subbase pavements, it is critical to collect construction data to identify potential risk factors that may limit pavement performance.

Construction methods, timing, material variance, and as-built quality could significantly influence pavement future performance (Tighe et al., 2007). Within this phase, major considerations include quality control procedures, uniformity of material or variation thereof, condition of roadbed, material placement, compaction activities and patterns used (Minde and Ghadge, 2018). In addition, LCC material strength and quality could be further influenced by pour thickness and pour interval (Liu et al., 2022). Likewise, environmental conditions during construction are crucial in setting up the platform for the pavement to either achieve its design life or fail prematurely. Temperature, moisture, solar radiation, and freeze-thaw cycles during construction and over the pavement's service life are important environmental conditions to watch for (Tighe et.al, 2007). It would be necessary to ensure that the pavement layers during construction are not exposed to more conditions than they can handle. Even if this happens, measures are already in place to mitigate damage such exposure could cause.

An ongoing research program that attempts to quantify the effect of construction activities on a pavement structure incorporating LCC and compare the performance with the traditional unbound material commonly used in Canada is described. The road segment is in Ontario and was designed and constructed by the University of Waterloo as part of the research programme. This paper briefly describes the test road facility and provides findings from the construction period. It is intended that data from this study would inform construction best practises when incorporating LCC within the pavement structure

## 2.0 Objective and Scope

A trial section with three different LCC densities was built to further examine the application of LCC in pavement construction and understand how it reacts and performs under varied conditions. The purpose of this study is to compare the behaviour of LCC pavements under construction loads and activities to that of standard granular subbase materials. This will aid future LCC applications, particularly in guiding construction decisions. Findings from this analysis will serve as a foundation for ensuring that the best possible performance is achieved when LCC is used as a subbase layer in the pavement structure. This paper describes the subsurface instrumentation and gives pressure, strain, moisture, and temperature data for these pavement sections during construction. This knowledge will additionally aid in explaining future performance and contribute to developing guidelines for LCC use.

### 2.1 Project Location and Design

The data for this study came from instrumentation deployed on a field section in St Agatha, Ontario, Canada, as part of an ongoing investigation that has seen the construction and instrumentation of new LCC subbase pavements. The design was for a minor arterial road based on an Annual Average Daily Traffic (AADT) of 6,349 vehicles per day, including 10 % heavy trucks, and was completed using AASHTO 93 and the Mechanistic and Empirical Pavement Design Guide (MEPDG).

The field trial segment consisted of four sections, each 50 meters long. For all sections, a consistent 100 mm of Superpave 19.0 (with 15% RAP) asphalt concrete (AC) was laid over 150 mm of granular A (GA) material as the base asphalt course. The finishing course is supposed to be 90 mm Superpave 12.5 asphalt concrete; however, at the time of this study, the layer had not been installed. The base and subbase layers of the control section are made of 300-millimetre-thick granular A material. The remaining three portions are known as LCC400, LCC475, and LCC600, and are each 200 millimetres thick Lightweight Cellular Concrete (LCC). The pavement was built on the same subgrade with a resilient modulus of 43 MPa.

However, the 400 and 475kg/m³ LCC portions had higher longitudinal slopes (≥1.1 %). In this investigation, the LCC material is made entirely of General use limestone cement with a cementitious/water ratio of 0.5. The asphalt concrete and Granular A were installed following the Ontario Provincial Roads and Public Works Standard (OPSS).

## 3.0 Methodology

### 3.1 Instrumentation Installation

Figure 1 shows a cross section of the pavement structure with the subsurface instrumentation at the test road facility. To get essential pavement strain responses, strain gauges were placed at the bottom of the surface and subbase. Pressure cells were put on top of the subgrade in each segment to acquire critical compressive stress at the top. Moisture and temperature sensors were also installed at the centre of each layer to determine the temperature and moisture profile within the pavement. 150 mm into the subgrade, moisture, and temperature sensors were also installed. Concrete maturity metres were set in the middle of all the LCC layers to measure the qualities of the LCC, particularly the curing period and full-strength gain duration after placement. The full instrumentation on this road was installed on the southbound outer lane. Two specialised data stations were built up on the side of the road to read and store data from the installed instrumentation.

Except for the surface layer asphalt installation, which followed a different technique, the installation followed the scheduled placement for each layer and a similar procedure stated in Oyeyi et al. (2019). Surface asphalt strain gauges were installed beneath the asphalt layer by first securing them with pegs and then burying the cables in granular A material. To thoroughly bury the sensor within the requisite thickness of the base course, a very thin layer of asphalt concrete was put beneath, around, and over it prior to the placement of the first asphalt concrete lift. During paving, to avoid damage to the sensors installed in the layer, the head of the paver was raised slightly when going over sensor locations
Figure 2 presents installed instrumentation on the field and some construction activities.

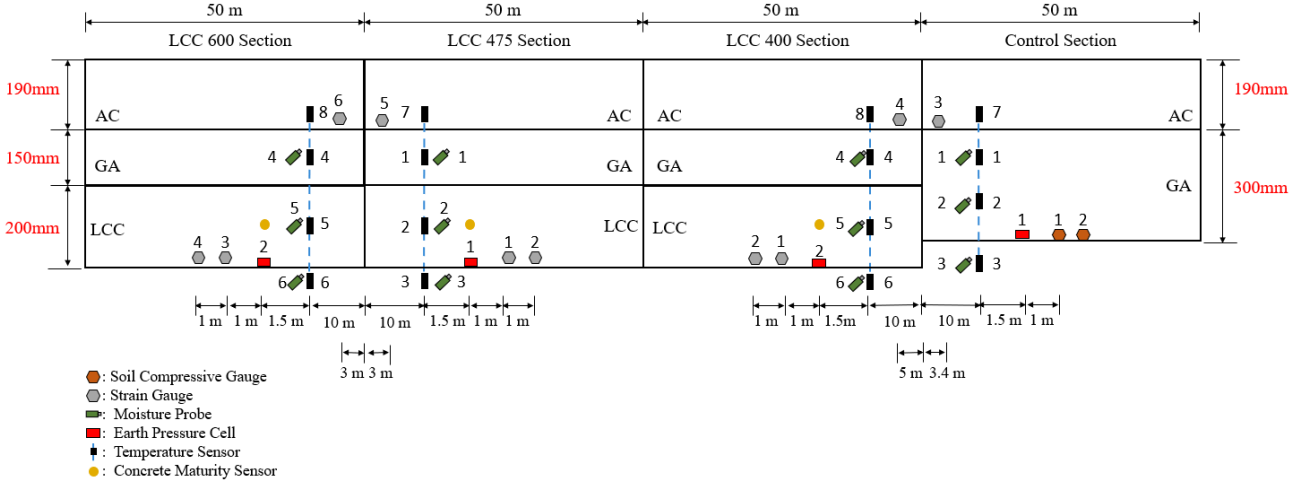


Figure 1: Pavement Section View with Instrumentation Location

### 3.2 Instrumentation measurements

The moisture sensors used in this study are like those described by Oyeyi et al. (2019) and use the same measurement techniques. The sensors' output data is Soil Water Potential (SWP), which shows water availability. The value of zero is obtained when the layer is fully saturated; the less water in the layer, the further away the measured value from zero. Equation 1 is used to convert measured resistance to a uniform basis of comparison by adjusting it to 21°C, and Equation 2 is used to convert the adjusted value to Soil Water Potential (SWP) in centibars (cb) units, which is equivalent to KPa (Henderson, 2012).

$$R_{21} = \frac{R_m}{(0.018(T_m - 21))} \quad (1)$$

Where,
$R_{21}$ is the resistance adjusted to 21°C.
$R_m$ is the resistance reading determined from the raw data collected by the CR1000 in kΩ.
$T_m$ is the temperature of the soil surrounding the moisture gauge in °C.

$$\text{SWP} = 7.407 \text{ x } R_{21} - 3.704 \quad (2)$$

Where,
SWP is the soil water potential measured in centibars (cb).

The temperature sensors were single point types that measured the temperature of each layer. The final SWP value was calculated by correlating the measured temperature in each layer with the moisture sensor. Each sensor is connected to the data recorder by a single-ended input channel and a voltage excitation channel, with each sensor taking measurements in degrees Celsius (°C) every ten seconds.

The earth pressure cells (EPC) are made up of a 3 K thermistor that uses the cell fluid viscosity characteristics to determine the pressure on the subgrade owing to applied load (Pickel et.al, 2018). A vibrating wire analyzer connects the EPCs to a data recorder, and measurements were taken every ten seconds.

The temperature within the LCC layers was associated with its compressive strength growth until 28 days to calculate the ultimate strength of the placed LCC using the maturity method. For each LCC density, one maturity sensor each was put in the center of two 150 x 300mm cylindrical specimens brought to the laboratory from the field. To avoid disrupting the material's structure, the specimens were kept undisturbed on the field for twenty-four hours before being moved. After 24 hours after casting, the specimens were placed in an 85 percent humidity room. The temperature recorded by the sensor within the specimen was compared to the results of 1, 3, 7, 14, and 28 days of unconfined compressive strength (UCS) to construct a maturity curve.

a. Overall view of installed sensors

b. LCC placement

c. Placing granular A around sensors on LCC

d. During asphalt paving operation

e. Data station

f. Completed road section

Figure 2: Instrumentation Installation and Construction Activities

ASTM C495 was used to conduct the unconfined compressive strength test. The specimens were left undisturbed for twenty-four hours before being moved and placed in an 85 percent humidity chamber, same as the maturity metre specimen. The UCS was calculated using equation 3.

$$\mathrm{UCS} = \frac{P}{A} \tag{3}$$

where:

UCS = unconfined compressive strength, MPa
P = maximum load recorded, kN
A = the cross-sectional area of the specimen, mm²

The datalogger read the nominal resistance of the strain gauge installed every 10 seconds by supplying an excitation voltage to the full bridge strain gauge. The measured voltage in microstrain units is the resultant value (Campbell Scientific, 2005).

## 4.0 Results

This section discusses installed instrumentation results concerning construction activities occurring within this period. Table 1 provides a summary of the construction schedule. Most sensors were installed in position on July 14, a day before the LCC pour, except the asphalt strain gauges which were place on the pavement the day of the asphalt paving, although the wiring was completed the same day as the other sensors.

Table 1: Construction Schedule

| Activity | Date |
|---|---|
| Instrumentation Placement | July 14, 2021 |
| Lightweight Cellular Concrete pour | July 15, 2021 |
| Granular A placement | July 19, 2021 |
| Curb and gutter/Sidewalk construction | July 29 - 30, 2021 |
| Asphalt paving and Asphalt Strain gauge installation | September 2 - 3, 2021 |
| Traffic opening | September 4, 2021 |

### 4.1 Concrete maturity

The ambient temperature during the LCC pours ranged between 20°C and 27°C, with no rainfall till two hours after the pour. Compressive strength results for 56 days are presented in Figure 3. Compressive strength increased over time and with an increase in density. By the third day, the LCC475 and LCC600 sections had surpassed the typical specified minimum 28-day compressive strength of 475 kg/m³ LCC of 0.5 MPa, according to Maher and Hagan (2016), is sufficient to support the pavement structure as a subbase material. The LCC400 sections surpassed this criterion by day seven. Figures 4a, b, and c, present the maturity curve for the LCC400, LCC475, and LCC600, respectively. The maturity curve was determined based on the strength and Temperature-Time Factor (TTF). This method determined that the ultimate strength to be achieved by the LCC400, LCC475, and LCC600 were 0.93 MPa, 1.25 MPa, and 2.08 MPa, respectively. These maximum strengths are nearly reached or surpassed by day 56, as shown in Figure 3.

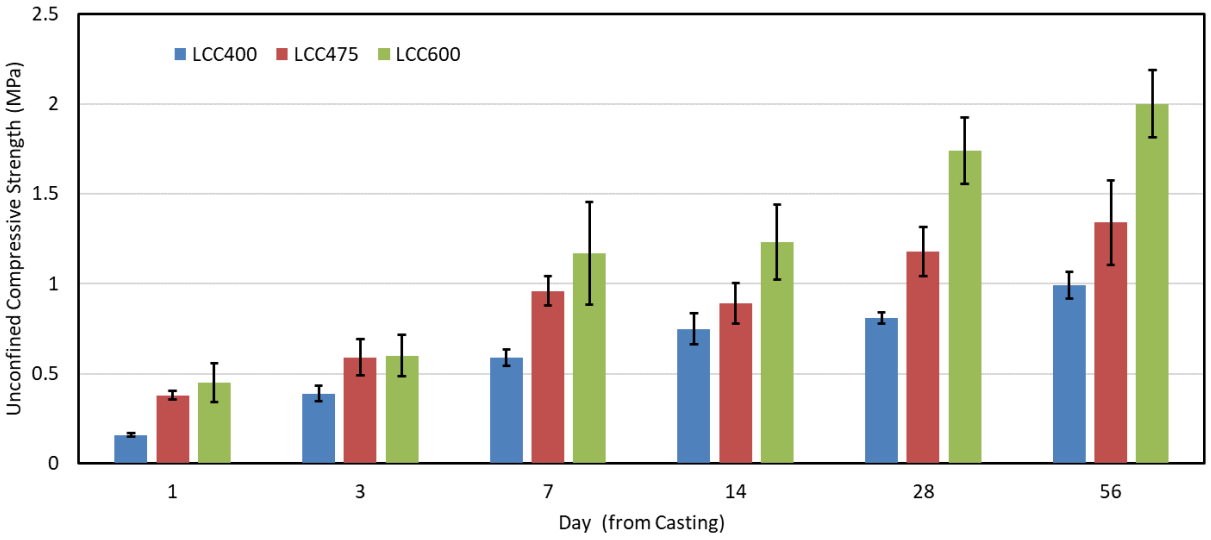


Figure 3: Compressive Strength of LCC

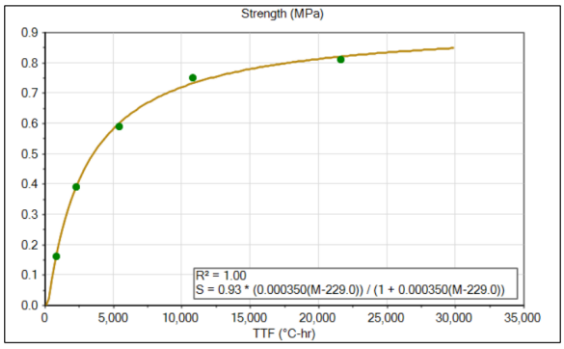


a. Maturity Curve for LCC400

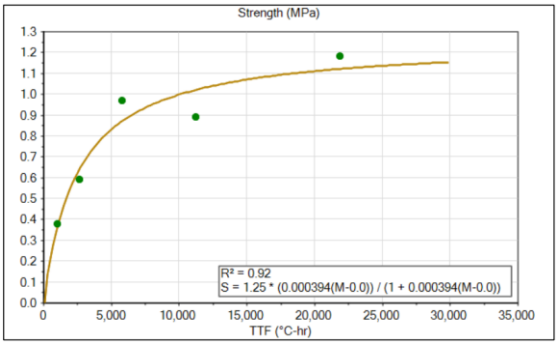


b. Maturity Curve for LCC475

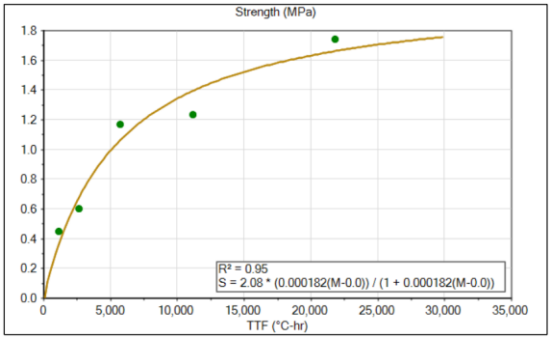


c. Maturity Curve for LCC600

Figure 4: LCC Maturity Curve

The temperature change during the first few hours of the casted LCC on the field is shown in Figure 5. The temperature within all the LCC layers reached their maximums within 5 – 9 hours from casting, with the

time to peak temperature decreasing with increased density. Peak temperatures were reached faster than 12 hours which is the typical time LCC could reach its peak temperature according to past studies (Tarasov et al., 2010). Tarasov et al. (2010) also noted that lower density LCC in thinner samples reached peak temperatures faster. The peak temperature within the LCC475 section was the highest and was 21% greater than the LCC400 section and 7 % more than the LCC600. The LCC600 temperature surpassed the LCC400 by 13%. According to Jones and McCarthy (2006), peak cellular concrete temperature was found to drop by 40% when cement quantity was reduced from 600 to 300 kg/m³. Generally, Volume of the pour, cement content, concrete density, and the amount, kind, and properties of the cement/filler/aggregate used are all factors that influence the hydration of LCC (Brady et al., 2001; Jones and McCarthy, 2006; Tarasov et al., 2010).

Furthermore, the time it takes for LCC to set is critical since it affects the construction schedule. Although there is no standard test technique for assessing the setting time of LCC, Brady et al. (2001) found that the ASTM C266 test method for cement could be used to determine the setting time of cellular concrete. The stiffening of cellular concrete has been seen after 5 hours of casting at 20 °C (Legatski, 1994). Results in this study reflect similar findings. Also, a significant temperature increase within the LCC was observed after the asphalt concrete was laid, with the LCC temperatures reaching another peak about 24 hours after the AC paving.

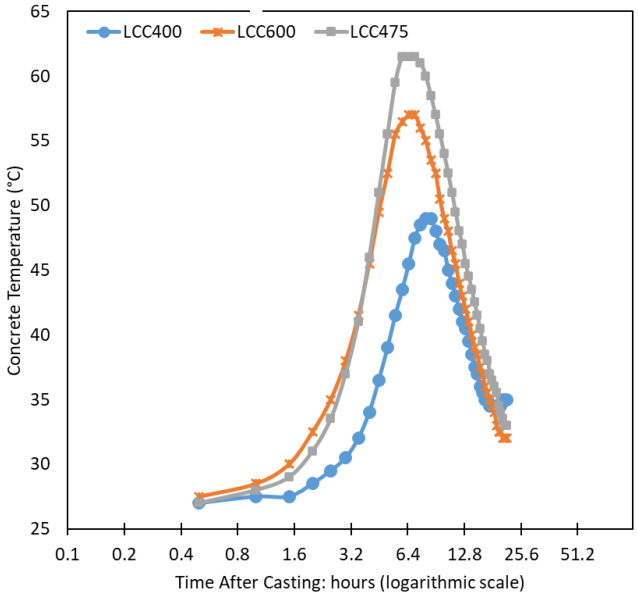


Figure 5: Temperature Profile of Lightweight Cellular Concrete Curing in the Field

Concrete maturity testing is beneficial as it could assist in monitoring LCC temperature and can be used to compare not only how LCC is curing but also to gauge the quality control of LCC. Results can be used to compare in-place concrete and cast cylinders. If the maturity estimates differ significantly from the cylinder samples, there may be a problem with the ready mix LCC. Knowledge of this aspect of the LCC material could help save construction time by determining how construction can progress following LCC pour (Jin et al., 2017).

### 4.2 Pressure

The dynamic pressure experienced at the surface of the subgrade during the construction period is presented in Figure 6. The analyses signify the change in pressure per time and do not reflect the change in pressure due to the subbase material itself. The figures show the dynamic pressure from the placement of the Granular A material (for LCC475 and LCC600) and some days after Granular A placement (For Control and LCC400) up until after the asphalt paving operation. The following observations have been noted.

Dynamic pressure as high as 7 KPa was noted at the LCC475 and LCC600 sections during the Granular A placement. Significant pressure change was observed during the curb /gutter and sidewalk construction. During this period, the control experienced the highest recorded dynamic pressure throughout the construction period of 97 kPa. In contrast, the LCC600 saw a 31 KPa pressure increase, the highest increase in this section throughout the construction period. LCC475 dynamic pressure this time was 18 kPa. The high-pressure amplitude at this time was likely due to the presence of heavy trucks carrying precast concrete blocks for the gutters and concrete mixers during the casting of the curbs. The LCC400 pressure cell stopped working during the curb operation, but the most pressure change noted in this section before this was 38 kPa at the start of the curb construction operation. A lower pressure reading at the LCC475 compared with LCC600 during curb construction could result from some of the heavy vehicles during this activity not going over the sensor location. On September 2 and 3, big pressure changes were also observed due to the asphalt paving operation constituting the asphalt paver and trucks delivering the asphalt concrete. The LCC475 section saw its highest pressure change of 31 kPa than any other construction activity. The greatest pressure changes in the control and LCC600 were 28 kPa and 20 kPa during the asphalt paving operation.

In summary, the control section was noted to experience 78% more pressure than the LCC600 and LCC475 and 61% more than LCC400 for the period the cell at this location was working during construction. The LCC400 section, most of the time, seemed to experience similar pressure levels as the control section going by the initial data available for the LCC400. Unfortunately, after roughly a month of use, the sensor became damaged. The asphalt paving operation appeared to cause 10% and 36% more dynamic pressure at the LCC475 section than the control and LCC600, respectively. The subgrade surface pressure decreased with increased LCC density at the different construction stages. When comparing the effects of vehicles, a significantly higher effect is observed during the construction of the sidewalk and curbs than the actual placement of the pavement layers for all the sections

Overall, construction equipment apparently causes a large amount of stress on the pavement subgrade and structure. There is also a significant time interval between the LCC pour and the placing of the AC layer. During this period, the LCC pavement saw a substantial amount of truck traffic, as seen by the pressure readings at the top of the subgrade, which were fairly high. It might be beneficial to have additional roadside works carried out before pouring the LCC layer to avoid significant damage to the pavement even before opening to traffic.

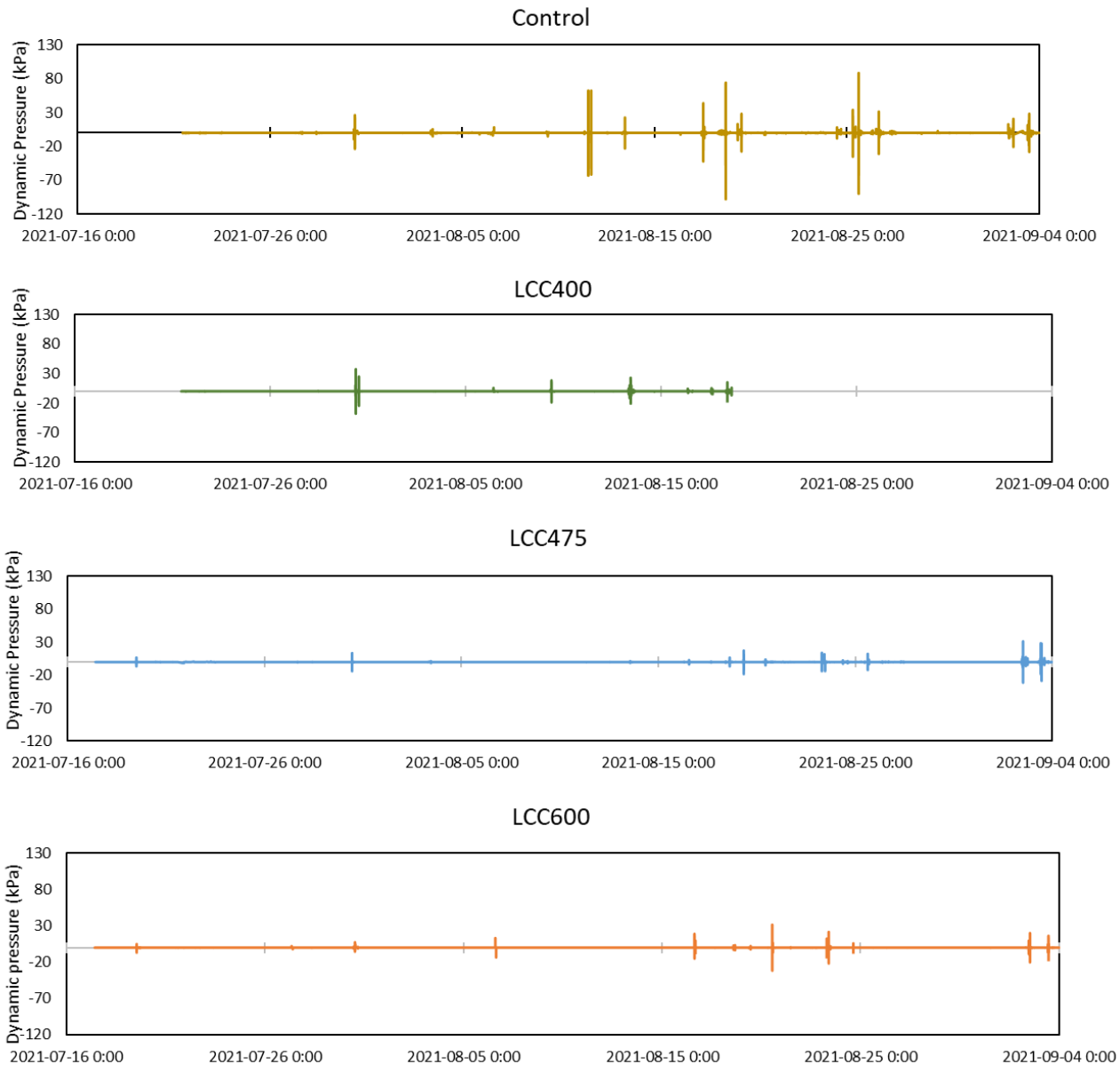


Figure 6: Subgrade Pressure During Construction

### 4.3 Moisture

Pavement moisture for all sections is illustrated in Figures 7 to 9. The layer is said to be fully saturated when the Soil Water Potential (SWP) is zero. The further away from zero the SWP, the drier the pavement layer. The direction of SWP is unimportant; only the absolute size of the value is considered.

The moisture profile of all the sections' base layers appears to follow the precipitation trend in the area. Rainfall times correspond with when most layers reflect SWP 0 or close to zero. The control sections' base appears to be constantly more saturated with water than the LCC sections. Although some draining is observed after rainfall events, the highest SWP value attained at the control section during the study period was 18 KPa. The LCC section base layer drains water faster and more after rainfall events. This is indicated by the peaks and troughs observed in the LCC sections. This drain is particularly higher and

noticeable in the LCC400 sections that show SWP as high as 148 KPa within the study period. The LCC475 and LCC 600 have shown SWP of 64 KPa and 25 KPa, respectively.

A similar trend is noted in the subbase, like the base layer, where the control section subbase layer depicts more saturated conditions than the LCC sections. Fluctuations with rainfall events are also observed. The LCC400 values appear to be mostly drier throughout the study period, with values close to 194 KPa observed. The LCC475/LCC600 station experienced technical problems during data collection, leading to some void readings. This is the reason for the blank spaces in the graph. However, when it read, the data indicated that the LCC475 sections sometimes contained less or no moisture than the LCC400 section. The LCC600 section, in some instances, appeared less saturated than the LCC 400 sections. Generally, the LCC475 and LCC400 subbase most times indicated lower moisture content than the LCC600 subbase.

The control sections' subgrade retains less water over the study period. However, the control subgrade still appears to have an average of 57 % more moisture than the LCC400 subgrade. Similarly, the LCC475 and LCC600 subgrades have lower moisture content than the control section, although more fluctuation is noted in these layers than in the others.

Largely, at the initial construction phases, more water draining from the pavement is noted, but a decrease is recorded over time, and more water is retained within the layers. This could indicate that further compaction of the pavement layers due to numerous truck traffic over extended periods of time without the asphalt concrete being placed, the drainage ability of the pavement layers could decrease, hence the potential for more water retention within the layers. This could yield challenges over time within the pavement structure. In addition, moisture content retention is seen to reduce with a decrease in LCC density. Optimising the LCC density to balance strength, moisture retention, and other properties might be necessary.

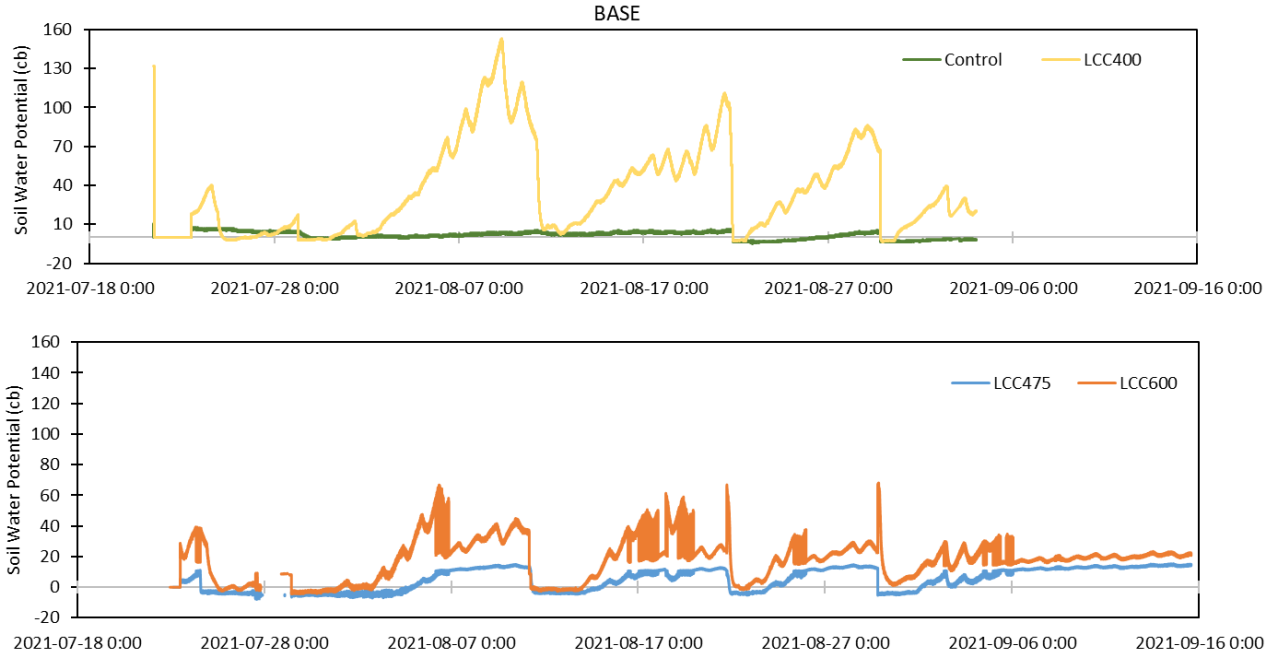


Figure 7: Base Moisture During Construction

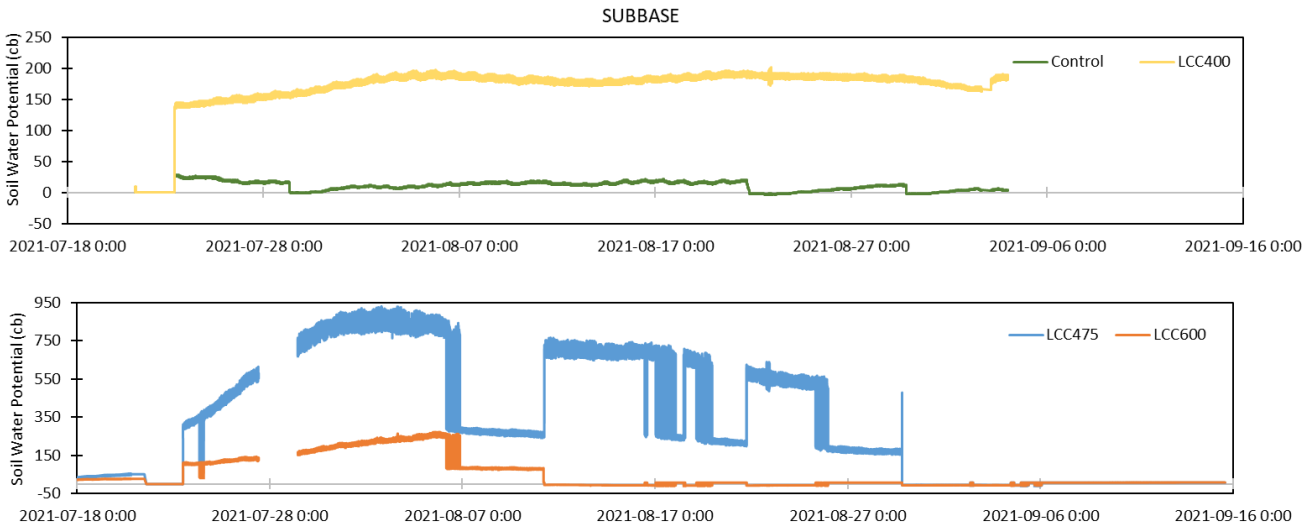


Figure 8: Subbase Moisture During Construction

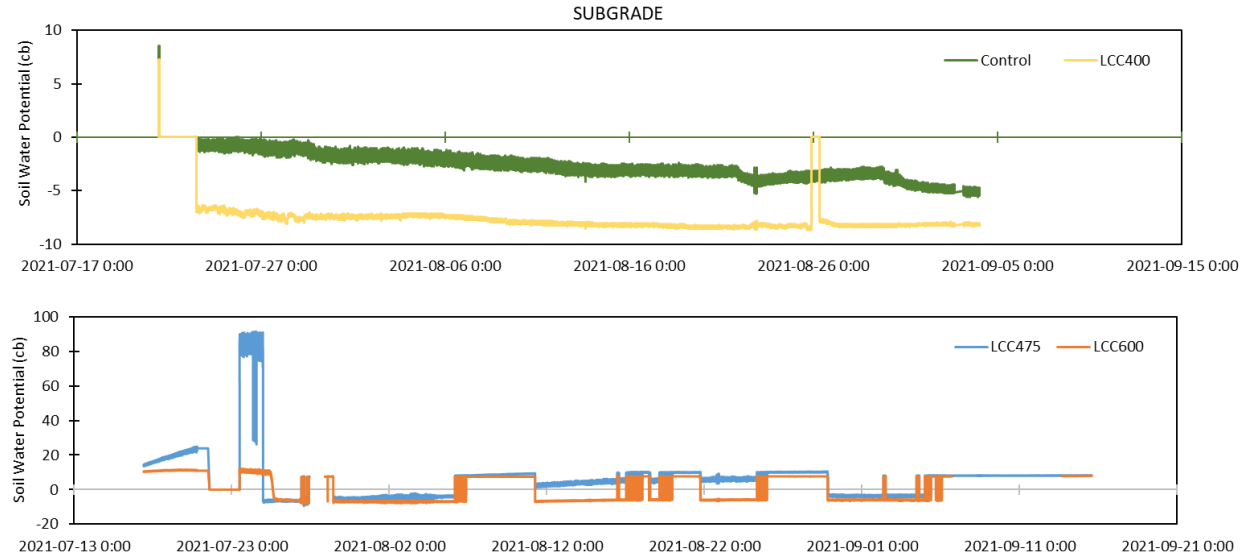


Figure 9: Subgrade Moisture During Construction

### 4.4 Temperature

Figures 10 to 12 present the temperature profile data for all sections and pavement layers during construction. The temperature trend is noted to correspond with ambient temperature in the location. The main temperature variation observed between the LCC sections and control asides from the initial placement of the LCC material and the effect of the heat of hydration (not noted in the figures) was 24 hours after the placement of asphalt concrete. The result was greater on the base and subbase layers in each section. The LCC layers appear to experience a 12% greater temperature increase in the base layers compared with the control. However, at the subbase, LCC400 experienced a comparable temperature increase to the control, but the LCC475 and LCC600 sections experienced 35% and 27% lower temperatures. While only minimal temperature increase of about 3°C was noted in the subgrade of LCC

475 and LCC600, 24% more temperature was observed in the control and 39 % more in the LCC400. After AC paving operation, the LCC400 layers were subjected to more significant temperature fluctuations, and its subgrade had a greater temperature increase. The different trend at this time compared to the other LCC sections could indicate a potential problem at this location when compared with results from other parameters such as moisture and pressure. A closer look needs to be taken to see if there is damage within the sections' layer.

Generally, the temperature profile for all layers in all the sections appears to follow a similar trend, especially for the base and subbase layers, and have a quite similar magnitude during the construction period except after asphalt paving. The control sections' subgrade experiences slightly higher temperatures than the LCC sections except for LCC400. Comparing LCC475 and LCC600, it appears that at ambient temperatures between 13°C and 33°C, the lower the LCC density, the lower the layer temperature. In addition, with an increase in pavement depth, a decrease in temperature is noted.

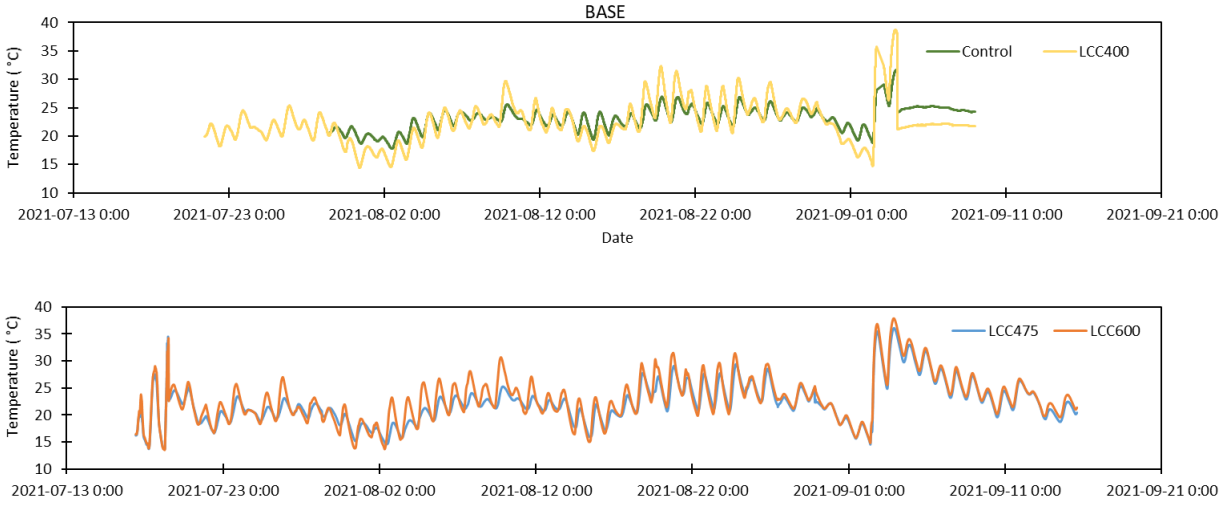


Figure 10: Base Temperature During Construction

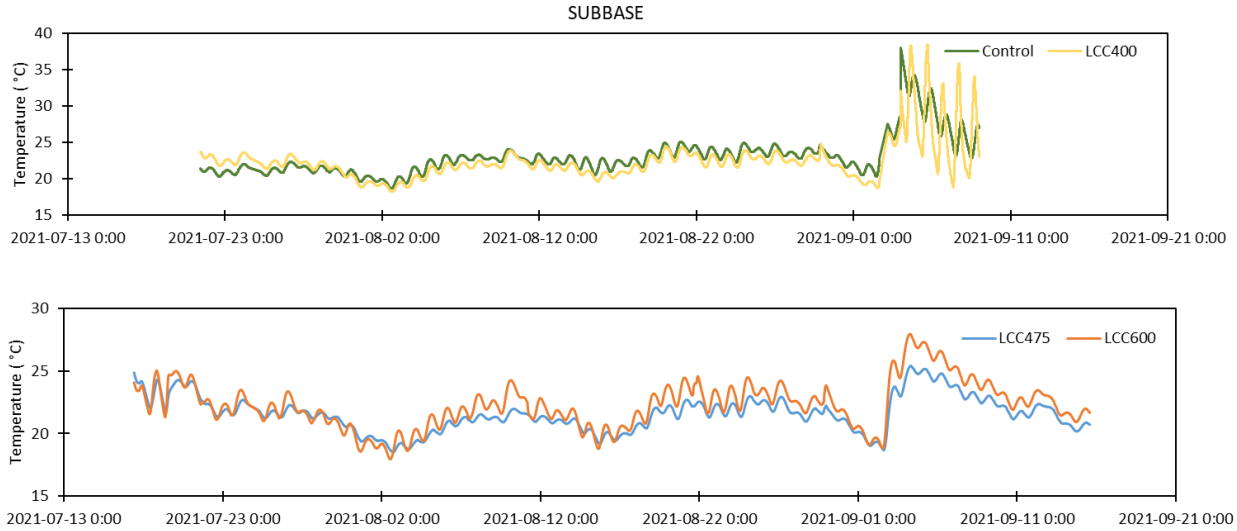


Figure 11: Subbase Temperature During Construction

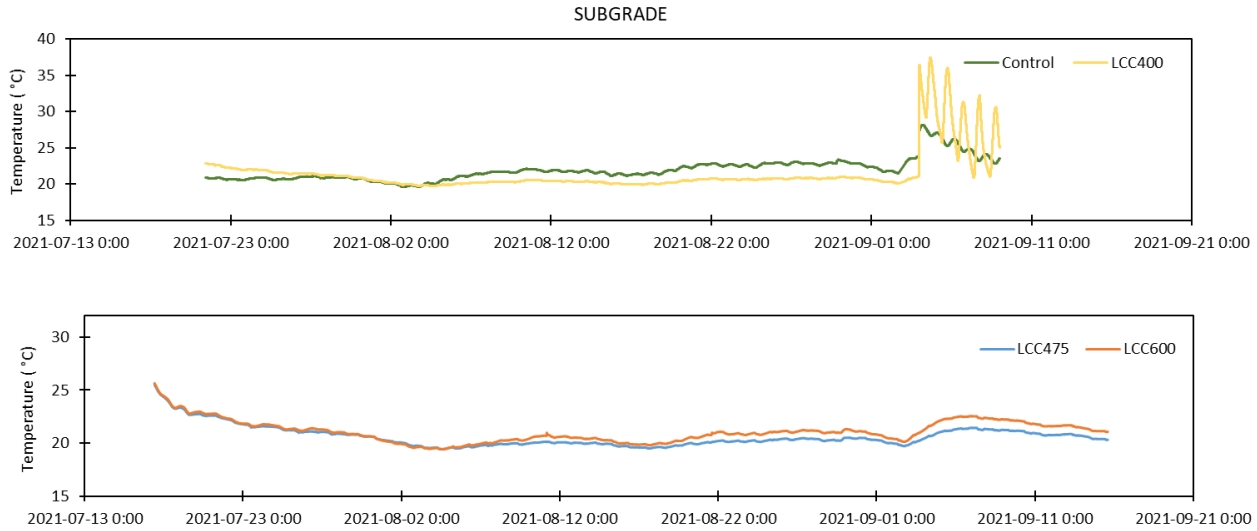


Figure 12: Subgrade Temperature During Construction

### 4.5 Strain Gauges

Dynamic longitudinal strain experienced beneath the asphalt layer is presented in Figure 13, while Figures 14 and 15 show the dynamic transverse and longitudinal strains beneath the subbase layers accordingly. During the asphalt paving operation, the LCC600 section was noted to experience nine times more strain than the control and three times more than the LCC400 and LCC475 sections beneath the asphalt layer. The LCC 475 and LCC600 saw three times more strain change than the control. The strain on the LCC400 was 15% more than LCC475. The magnitude of the strains at this location could be because of the concentration of truck traffic within the LCC475 and LCC600 sections. The paver also had a waiting period at this location during the paving operation.

At the bottom of the subbase, during the granular A placement, dynamic transverse strain of 287με was seen at the LCC475 portion, while LCC600 experienced 42με. No strain value was available for control and LCC400 during granular A placement. During the curb and gutter installation, the LCC475 and LCC600 sections appeared to experience higher dynamic strains than the control and LCC400. The strain values are noted to increase with LCC density during this time. The maximum strain in the LCC600 section was 25% more than LCC475, 70% more than LCC400, and 83% more than the control. Likewise, during asphalt paving, the dynamic strain magnitude was minimal (Between 1 and 4 με) for control and LCC400; however, significant in LCC600 with a peak value of 181με and LCC475 234με. The Asphalt paver stayed at the location for a while and was not moving, it was moving at the other location. A reduction in transverse strain magnitude of 78%, 46%, and 84% were seen with increased pavement depth from beneath the surface layer to the subbase layer at the control, LCC475, and LCC600 sections, respectively.

Conversely, longitudinal dynamic strains at the bottom of the LCC475 and LCC600 were three and two times less in LCC475 and LCC600 than the transverse strains, respectively. The magnitude for all the LCC sections appeared to be within a similar range of 0 - 50 με most of the time. However, at some point, the LCC475 section appeared to have 74% more strain change than LCC400 and LCC600 sections. Unfortunately, the longitudinal strain in the control section was not responding to changes during this period. Also, strain gauges in LCC475 and LCC600 were faulty between 27 and 29 July.

Mostly, construction activities seem to impact greater strains on the LCC pavements than the unbound granular pavement. This is especially true beneath the asphalt layer during paving operations and

placement of granular A material. The magnitude of the strain change beneath the asphalt layer during paving increased with increased density. The impact of the asphalt paving operation is not noticed beneath the subbase layers in the control and LCC400 sections. Strain magnitude reduced with pavement depth, and the LCC600 density seemed to reduce strains at the bottom of the subbase layer the most.

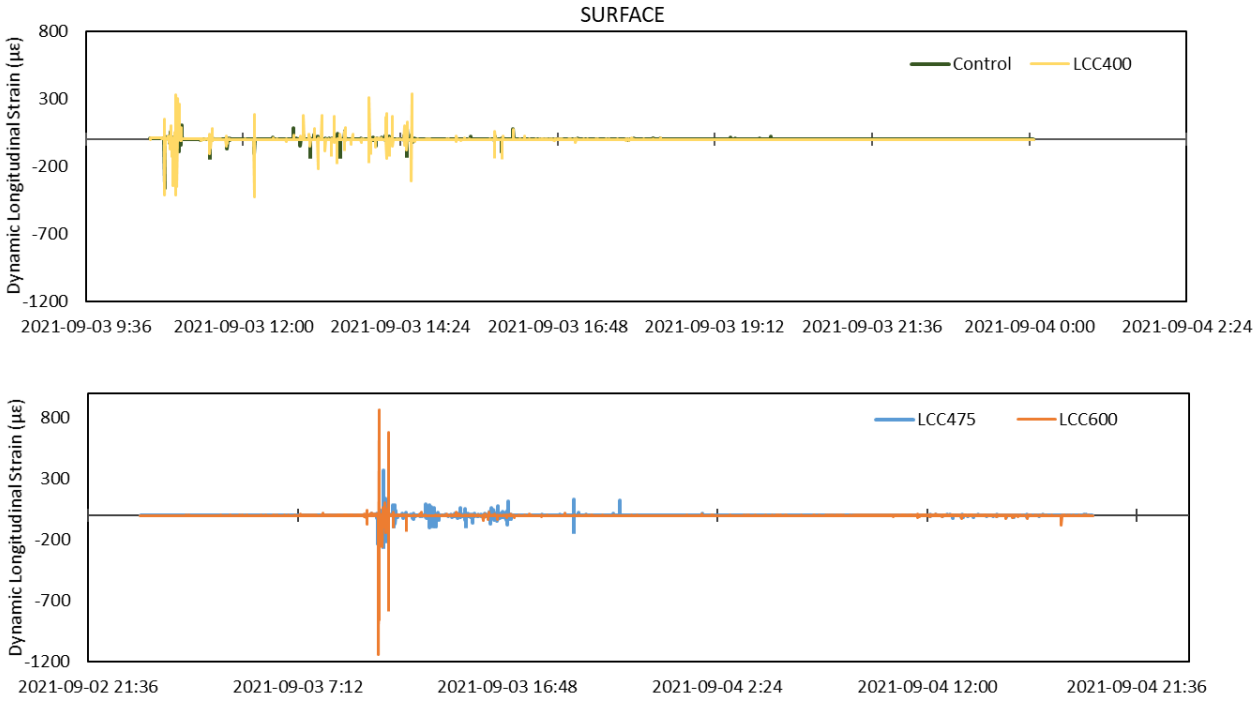


Figure 13: Dynamic Strain Beneath Surface Layer

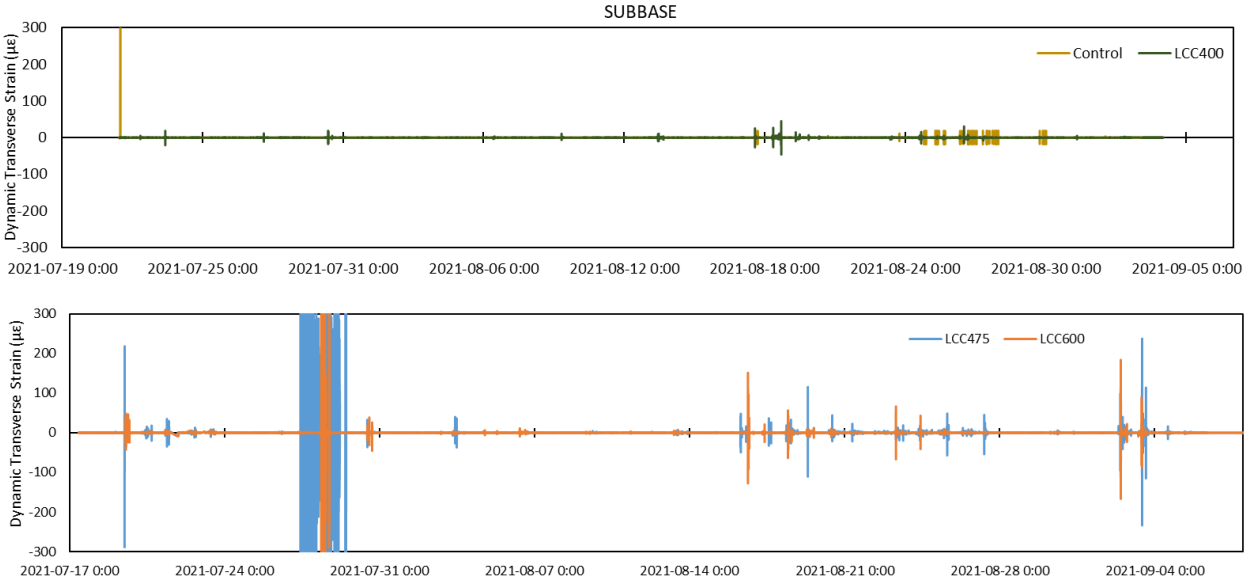


Figure 14: Dynamic Transverse Strain Beneath Subbase Layer

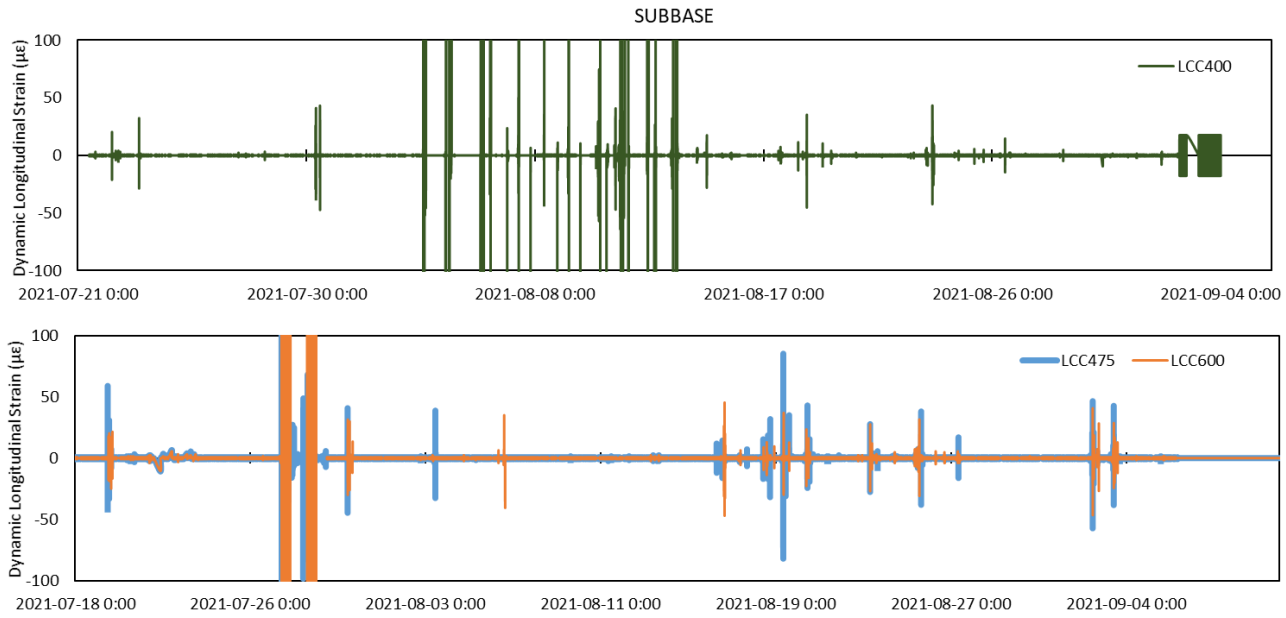


Figure 15: Dynamic Longitudinal Strain Beneath Subbase Layer

## 5.0 Conclusions and Recommendations

The practicality of adding three different densities of Lightweight Cellular Concrete in the subbase of flexible pavements was investigated in this study. The study area was located in St. Agatha, Ontario. In-situ pressure, strain, moisture temperature, and concrete performance during construction were compared to a typical pavement system with a subbase layer of unbound granular material. The results can be summarized as follows.

- The 475 kg/m³ and 600 kg/m³ density layers by day three and LCC400 by day seven had surpassed the typical specified minimum 28-day compressive strength of 0.5 MPa, indicating that the layer has sufficient strength to support the pavement structure as a subbase layer. Predicted ultimate strengths were found to be 0.93 MPa, 1.93 MPa, and 2.08 MPa for the three densities.

- 400 kg/m³, 475 kg/m³, and 600 kg/m³ density LCC incorporated as a subbase layer can reduce subgrade pressures by up to 78% compared with granular material during construction.

- All three LCC densities have a setting time between 5 to 9 hours. The temperature within the LCC pavements became cooler over time with increased density during construction.

- LCC subbase does not hinder the drainage ability of the pavement structure and causes the base layer to drain water more than the granular alternative during construction.

- High dynamic strain responses could be present at the surface and subbase of LCC pavements before asphalt paving compared with unbound granular material.

- The dynamic strain reduced with an increase in pavement depth when granular and LCC materials were used as subbase. This strain reduction was the most when a 600 kg/m³ density LCC layer was applied as pavement subbase.

- Excessive vehicles and trucks over the LCC pavement sections before asphalt paving could be detrimental to LCC pavement performance by inducing higher strains, leading to early cracking and weakening of the LCC layer. Avoiding excessive truck and vehicular traffic on LCC sections

before asphalt paving could be helpful. Alternately, the roadway design structure could be modified to allow for the anticipated vehicular loads prior to asphalt placement. Modification of the design to accommodate construction and other vehicular traffic must consider site-specific subgrade conditions and could involve increasing the LCC and/or granular base course thicknesses.

- In addition, limiting the duration between LCC pour and asphalt paving operations could help reduce the problems present due to vehicular traffic.

## 6.0 References


Averyanov, S. (2018). *Analysis of construction experience of using lightweight cellular concrete as a subbase material* [University of Waterloo]. http://hdl.handle.net/10012/13731

Brady, K. C., Watts, G. R. A., & Jones, M. R. (2001). *Specification for Foamed Concrete*. https://doi.org/PR/IS/40/01 TF 3/31

Decký, M., Drusa, M., Zgútová, K., Blaško, M., Hájek, M., & Scherfel, W. (2016). Foam Concrete as New Material in Road Constructions. *Procedia Engineering*, *161*, 428–433. https://doi.org/10.1016/j.proeng.2016.08.585

Henderson, V. (2012). *Evaluation of the Performance of Pervious Concrete Pavement in the Canadian Climate*. University of Waterloo.

Jin, N. J., Yeon, K. S., Min, S. H., & Yeon, J. (2017). Using the Maturity Method in Predicting the Compressive Strength of Vinyl Ester Polymer Concrete at an Early Age. *Advances in Materials Science and Engineering*, *2017*. https://doi.org/10.1155/2017/4546732

Jones, M. R., & McCarthy, A. (2006). Heat of hydration in foamed concrete: Effect of mix constituents and plastic density. *Cement and concrete research*, 36(6), 1032-1041.

Legatski, L. A. (1994). "Cellular Concrete," STP36448S Significance of Tests and Properties of Concrete and Concrete-Making Materials. In P. Klieger & J. Lamond (Eds.), *ASTM International* (Issue 1). https://doi.org/STP36448S

Maher, M. L. J., & Hagan, J. B. (2016). *Constructability benefits of the use of lightweight foamed concrete fill (lfcf) in pavement applications*. Canadian Society for Civil Engineering Annual Conference 2016: Resilient Infrastructure, 2, 1354–1362. https://www.scopus.com/inward/record.uri?eid=2-s2.0-85030676066&partnerID=40&md5=bc7a95ed0e09ae483ebab9e6540d0c8a

Ni, F. M.-W., Oyeyi, A. G., & Tighe, S. (2021). Structural capacity evaluation of lightweight cellular concrete for flexible pavement subbase. *Road Materials and Pavement Design*, *0*(0), 1–17. https://doi.org/10.1080/14680629.2021.1999844

Oyeyi, A. G., Ni, F. M.-W., Pickel, D., & Tighe, S. L. (2019). *Lightweight Cellular Concrete as a Subbase Alternative in Pavements: Instrumentation plan, Installation and Preliminary results*. Proceedings of Transportation Research Board 98th Annual Meeting. Washington D.C., United States https://www.tac-atc.ca/sites/default/files/conf_papers/oyeyi_a-

lightweight_cellular_concrete_as_a_subbase_alternative_in_pavements_instrumentation_plan_installation_and_preliminary_results-v2.pdf

Pickel, D. J., Tighe, S. L., Lee, W., and Fung, R. 2018. "*Highway 400 Precast Concrete Inlay Panel Project: Instrumentation Plan, Installation, and Preliminary Results*." Proceedings of Transportation Research Board 97th Annual Meeting. Washington D.C., United States:

Rahul R. Minde and Anil N. Ghadge (2018). *Analysing the factors influencing quality throughout the life cycle of a road project.* 3rd International conference on Construction, Real estate, Infrastructure and Project management. (ICCRIP 2018). Pune. November 2018

Tarasov, A. S., Kearsley, E. P., Kolomatskiy, A. S., & Mostert, H. F. (2010). Heat evolution due to cement hydration in foamed concrete. *Magazine of Concrete Research*, *62*(12), 895–906. https://doi.org/10.1680/macr.2010.62.12.895

Tighe, S., Falls, L. C., & Doré, G. (2007). Pavement performance evaluation of three Canadian low-volume test roads. *Transportation Research Record*, *2*(1989), 211–218. https://doi.org/10.3141/1989-66

Tiwari, B., Ajmera, B., Maw, R., Cole, R., Villegas, D., & Palmerson, P. (2017). Mechanical Properties of Lightweight Cellular Concrete for Geotechnical Applications. *Journal of Materials in Civil Engineering*, *29*(7), 06017007. https://doi.org/10.1061/(ASCE)MT.1943-5533.0001885